

New Approach for the Root Cause of Fukushima Meltdown Accident

Tsuyoshi Matsuoka

Mechanical Engineering, Kyushu University, Kobe City, Japan

Email address:

matsuoka-tsuyoshi@nifty.com

To cite this article:

Tsuyoshi Matsuoka. New Approach for the Root Cause of Fukushima Meltdown Accident. *International Journal of Science, Technology and Society*. Vol. 11, No. 2, 2023, pp. 62-73. doi: 10.11648/j.ijsts.20231102.14

Received: December 5, 2022; **Accepted:** January 11, 2023; **Published:** March 21, 2023

Abstract: The purpose of this Commentary is to clarify as much as possible the whole history of reactor and containment pressure changes in the Fukushima meltdown accident. It is based on a new approach for film boiling, which is kept after the Zr-H₂O reactions. Most important point of this approach is that the author applied film boiling based on boiling curve, which is basic theory in boiling phenomena, for the Fukushima accident phenomena. As the reaction rate is proportional to the reactor or containment pressure under film boiling, it increases rapidly and stops suddenly, keeping the film boiling. The containment pressure change consists of three phases, namely pressurizing, keeping the high pressure and de-pressurizing. The containment is pressurized by H₂ gas and steam produced by the Zr-H₂O reactions and de-pressurized by a heatsink such as the containment wall and inner shield concrete after reaction stops. The high pressure between these pressure changes is kept by balancing the H₂ gas produced by reaction with the leaked gas from the gap between the top lid and the containment. Core decay heat is large, but its change is negligibly small. So, the pressurization is calculated from H₂ gas and steam produced by the Zr-H₂O reactions. The heatsink balances with the reaction during the high pressure condition. The de-pressurization occurs after the reaction is over, so the reaction heat rate can be calculated by the heat rate of the heatsink, which is equal to the condensation rate during de-pressurization. The leak rate of the leak gas can be calculated using the reaction rate. It is very important that the reaction rate is slowed by the insufficient steam supply, as the melted reactor cores in the Fukushima accident were covered with H₂ gas and steam (film boiling) at 0.8MPa or lower pressure. This is different from the rate (at approx. 7MPa) in the Three Mile Island accident, as the steam specific volume at 0.8 MPa is ten times larger than that at 7 MPa. The calculation results based on this assumption show that almost all the Zr in each core of Units 1, 2 and 3 reacted with water.

Keywords: Fukushima Daiichi Nuclear Power Plant, Meltdown, Boiling Curve, Film Boiling, Steam Condensation, Zr-H₂O Reaction, Containment Pressure

1. Introduction

About 10 years have passed since the Fukushima meltdown accident began on March 11, +2011. Since then, TEPCO (Tokyo Electric Power Company, Inc.) has been reviewing and researching the root causes of the accident and published its 5th Progress Report (<https://www.tepco.co.jp/en/decommission/accident/unsolved-e.html>) "The investigation and review report of unconfirmed and unresolved issues on Fukushima meltdown accidents" on December 25, 2017 [1]. The author independently reviewed this report and concluded as follows: after the Zr-H₂O reactions occurred, the boiling state in the reactor core should be presumed to be film boiling. As shown in the boiling curve

[2] of Figure 1, once the boiling is changed to film boiling, the film boiling can continue using only the decay heat. The 5th Progress Report did not discuss the accident from this viewpoint. Using this viewpoint, the author has been able to give good explanations for almost all unresolved items in the Progress Report, and this new approach gave better fits to the measured data of reactor pressures and containment pressures and the dose rates at the site and neighboring points. Though "the agreement between the NUCLEA (thermodynamic database) predictions and the results of experiments indicate that thermodynamic equilibrium phases play an important role in governing the core damage progression" [8], there are no discussion or review reports about the relation between Zr-H₂O reactions and "film boiling" such as the new approach

in this paper [9-15]. As for film boiling, the Commentary is made visually understandable by viewing the You Tube site “RHNB-Water (Slow Motion Playback)” and referring to the menu item “Bigger Red Hot Nickel Ball in Hot Water” for which the “Red Hot Nickel Ball” is seen as a reactor core. Just

after the Red Hot Nickel Ball was thrown into the cup, there was no increase of boiling. This means film boiling occurred. This means also that pressure increase in Reactor Core did not occur by relocation but by Zr-H₂O reactions. This is the most important point.

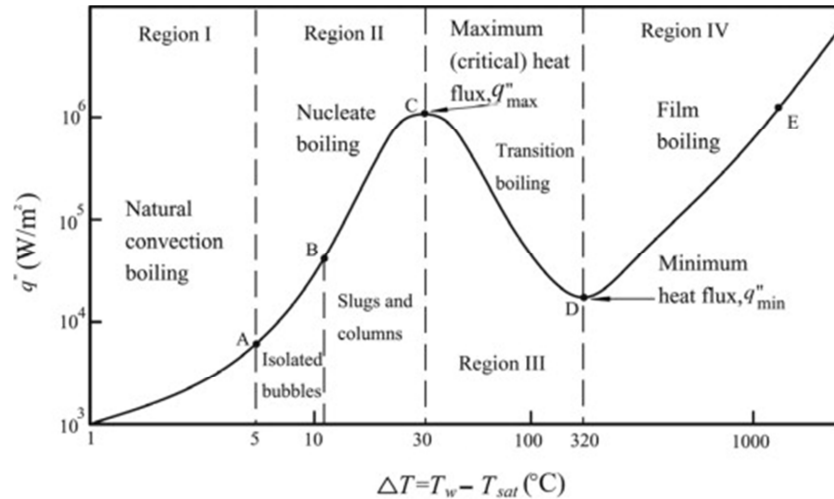


Figure 1. Boiling Curve [2].

2. Analysis and Review of the Reactor and Containment Vessel Pressure Changes

After the loss of core cooling function (for the permanently installed equipment) of Units 1, 2 and 3, it was understood that water injection from an external plant source to the core must be tried as a final means for dealing with the severe accident. However, in the Fukushima Daiichi Nuclear

Power Plant, water injection to the unit cores was done under the worst conditions of long term blackout, mountains of rubble caused by the Great East Japan Earthquake and Tsunami and occurrence of further frequent aftershocks. Furthermore, for Units 2 and 3, there was the additional burden caused by the hydrogen explosions of the neighboring Units 1, 3 and 4. To inject water into the core, the safety relief valve (SRV) should be opened to depressurize the core, and the saturated steam in the core should be discharged to the S/C (Figures 2, 3, 4 and 5) [1].

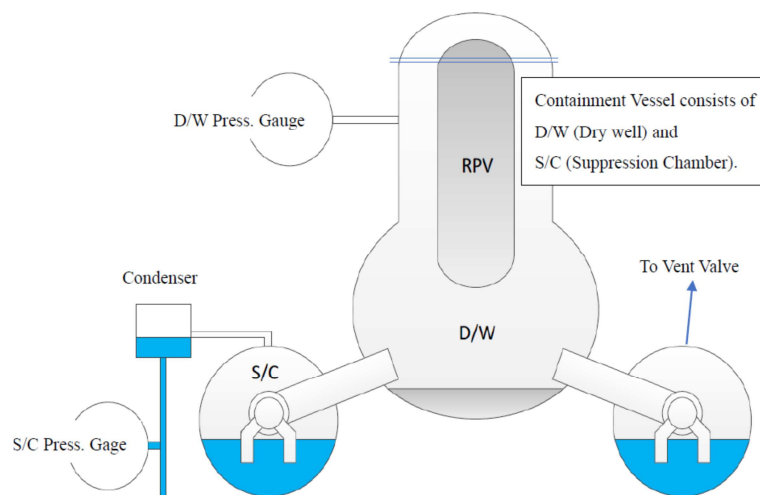


Figure 2. Containment Vessel [1].

Due to high back pressure (containment pressure) of the SRV, the SRV could not be opened using the regular procedures. Its opening procedures were very hard work, and more than 6.5 h were needed in opening the SRV of Unit 3.

On the other hand, the core of Unit 2 could be depressurized. However, unexpected interruptions against core cooling took place during water injection to the core by a fire engine. And moreover, the venting valve for depressurizing the

containment vessel located on the top of the suppression chamber (S/C) could not be opened due to its “Fail Close” design. During these processes, the reactor cores of Units 2 and 3 were heated by the decay heat, water in the reactor core was evaporated, and then the fuel rods were exposed to steam, and temperature of these fuel rods rose significantly in a short time. Then, unexpected events happened due to the water injection. The fuel rods were broken, and the Zr-H₂O reactions occurred. The reactor cores were heated further and melted. Hydrogen gas was generated by these reactions and hydrogen explosions occurred. The pressure transitions in the reactor and containment vessels showed typical phenomena and progression in these processes.

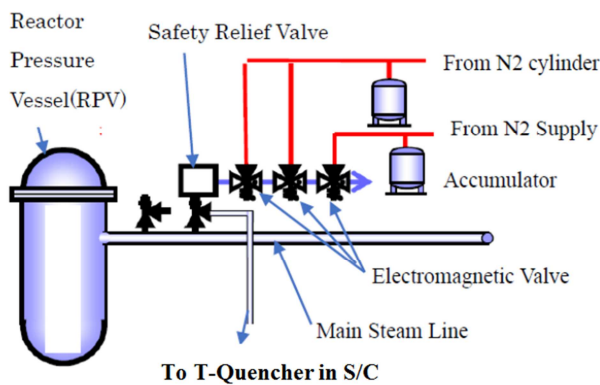


Figure 3. Safety Relief Valve (SRV) [1].

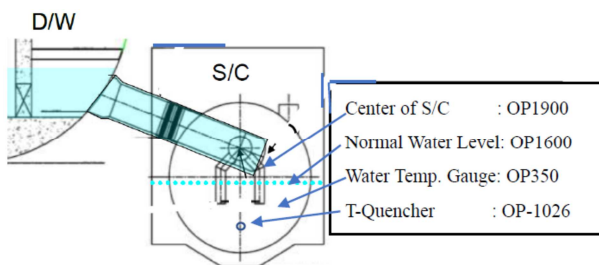


Figure 4. Steam Discharge (T-Quencher) Level and Water Level in S/C [1].

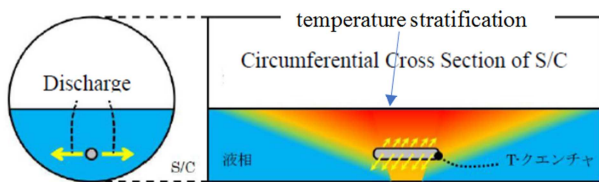


Figure 5. Steam Discharge (T-quencher) from SRV [1].

Hereafter, the author takes the unique viewpoint, not taken by TEPCO's 5th Progress Report, that once the boiling is changed to film boiling, the film boiling can continue using only the decay heat and uses it to analyze and review the accident. Hereafter, information quoted from the 5th Progress Report is presented in quotation marks as the author's English translation of the original Japanese.

2.1. Analysis and Review of the Reactor and Containment Vessel Pressure Changes

In TEPCO's 5th Progress Report, the major factors

resulting in changes of containment pressure after Zr-H₂O reactions were that “under core decay heat, de-pressurization was occurring by opening of a vent valve and pressurization was occurring by closing of that valve. Many opening and closing timings of the vent valve are described as ‘assumption’ because of no records”. So, based on the above unique viewpoint, the author analyzed, evaluated, and reviewed the reactor and containment pressures among the many available measured data in Units 1, 2 and 3 (Figures 6, 7, 8 and 9). In these figures, the state of melting cores and the phase of boiling curve of Figure 1 are added, based upon the new approach with this unique viewpoint.

(1) Fundamental approach

When the Zr-H₂O reactions occurred, hydrogen gas and superheated steam generated by the reactions were routed to the SRV line and passed through water (lower portion) and gas (upper portion) in the S/C to the drywell (D/W) (Figures 2, 3, 4 and 5). Hydrogen gas (high temperature) moved upward with nitrogen gas that initially filled the containment vessel (including the D/W and S/C). And then, while the steam was dissipating, the condensing heat was being transferred to the wall surface and the nitrogen gas, while the steam-rich mixed gases moved upward. Hydrogen-rich mixed gases were in the upper portion and the steam-rich mixed gases were in lower portion of the containment vessel. The hydrogen-rich mixed gases were released when the lid of the D/W was lifted slightly, and after some time elapsed, the containment vessel was filled with the residual steam-rich mixed gases. When the Zr-H₂O reactions ceased in this condition, de-pressurizing of the containment vessel started. It was presumed that the de-pressurization proceeded at an accelerated speed due to the dissipation of heat transferred to the containment vessel wall and of the condensing heat to the mists, and the pressure and temperature fell to the de-pressurized boiling point of the condensed water in the D/W and of the saturated water near surface in the S/C, respectively. As for the relationship of decay heat and the Zr-H₂O reaction heat in the reactor core, at first, it should be considered that the reactor pressure was balanced by the containment pressure with only decay heat (without Zr-H₂O reaction heat) after the SRV was opened. And then, it should be considered that containment pressure was changed by the Zr-H₂O reactions in the damaged reactor core. As for the decay heat and/or reaction heat, they should consist of the sensible heat of injection water, the latent heat by vaporization and the heat from increasing and decreasing the steam pressure. If the heat per their unit weight is considered, the latent heat (2200 kJ/kg at 0.2 MPa and 2100 kJ/kg at 0.5 MPa) has the largest effect, the sensible heat of 500 kJ/kg from 20°C (150 kJ/kg) to the saturated temperature (650 kJ/kg) has the second largest effect, and this sensible heat change becomes small after completion of temperature stratification shown in Figure 5. The heat from increasing and decreasing pressure (40 kJ/kg with the pressure rise from 0.2 MPa to 0.5 MPa) has the smallest effect. On the contrary, these phenomena indicate that the containment pressure is highly sensitive to “the heat input from increasing and

decreasing steam pressure". Before the Zr-H₂O reactions, based on mass balance, the amount of saturated water in the S/C increases in proportional to the amount of core injection water. Based on heat balance, the decay heats are balanced with the heat from increasing and decreasing steam pressure, the dissipated heat from the containment vessel wall and the sensible heat of the injection water. If the heat per unit weight is considered, most of the evaporated steam was condensed and became saturated water, and a very small part

contributed to the steam pressure change. On the other hand, when the reactions started, the film boiling took place around the high temperature (melted) fuel rods. So, the injection water changed suddenly to superheated steam. The superheated steam and the high temperature hydrogen were cooled by the injection water in the reactor core and by mixing with the S/C water, and then they became saturated steam and high temperature hydrogen which were then released from the water surface in the S/C.

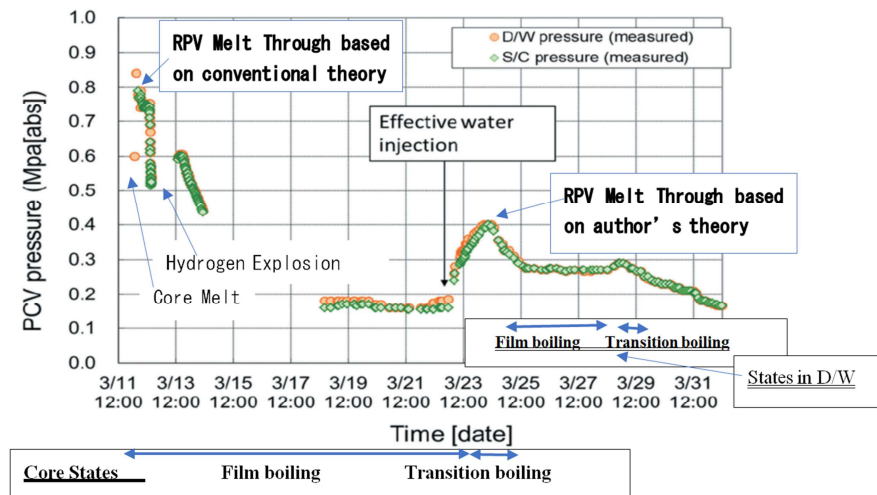


Figure 6. Containment Pressure and State of Core on Unit 1 [3].

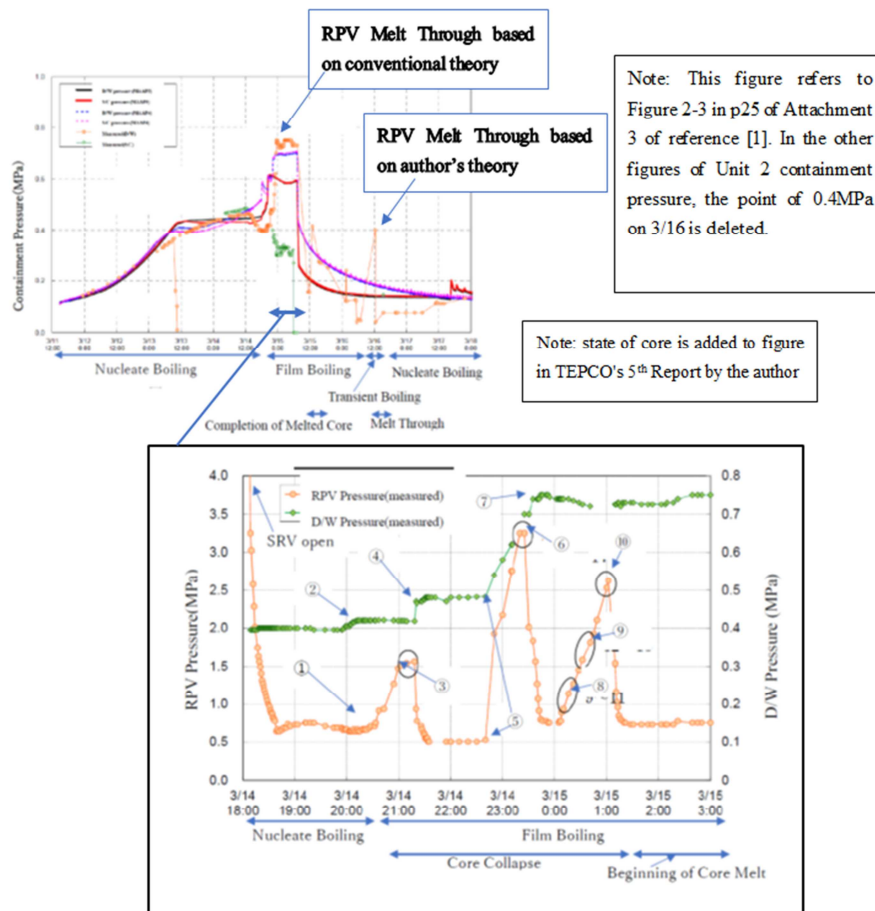


Figure 7. Reactor and Containment Pressure and State of Core of Unit 2 [1].

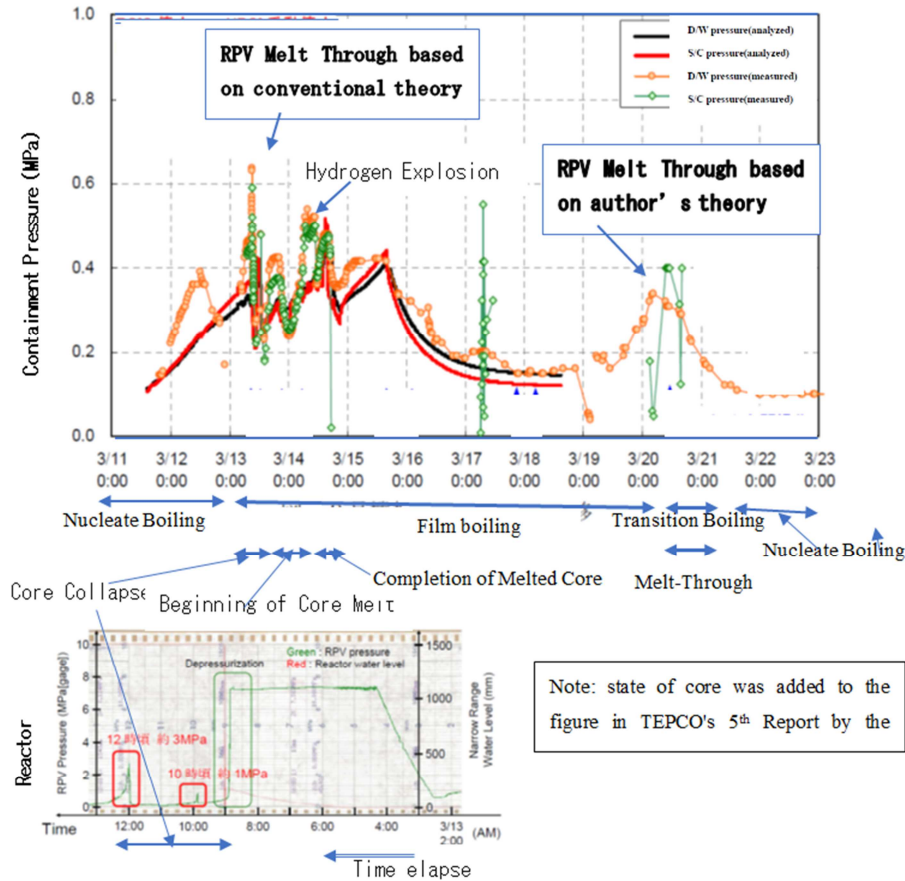


Figure 8. Reactor and Containment Pressure and State of Core of Unit 3 [1].

Since the temperatures of the mixed water in the S/C were not higher than the saturated temperatures, the Zr-H₂O reaction heat was changed finally to “the heat input for steam pressure rise”. Eventually, the pressure changes in the containment vessel were dominated by the Zr-H₂O reaction heat. The Zr-H₂O reactions that occurred in the Fukushima accident took place at about 0.7 MPa and this accident has been frequently compared with the Three Mile Island (TMI) accident that also took place at about 7.0 MPa. As the steam specific volume (0.24 m³/kg) in the Fukushima accident was 10 times larger than the volume (0.027 m³/kg) in the TMI accident, the restriction of up-flow (volume flow) increased remarkably, and so the mass flow was also reduced remarkably in the Fukushima accident. And the TMI accident was ended with the forced circulation achieved by operation of the main coolant pump. However, the Fukushima accident was ended with natural circulation by pool boiling. The Zr-H₂O reactions are completed within a second under the high temperature condition. But the amount of the reactions is determined by the amount of steam. The fuel rods and/or melted mixtures were engulfed by hydrogen and steam, which consisted of down-flow to the melted core and up-flow from the melted core. Consequently, the reactions continued long term because of the shortage of steam that could be supplied to the melted core, so-called, “slow and long-term reactions”. If it is assumed the flow rate of the generated steam and hydrogen was restricted by the SRV line (defined

as “restricted flow” in this paper), the amount of the reactions was proportional to the “restricted flow”. The mass flow rate [4] of superheated steam through a valve can be calculated from the valve C_v thanks to the following formula (1):

$$m = F_L \cdot C_v \cdot P_1 \cdot (y - 0.148y^3) / (83.7(1 + 0.00126 T_{sh})) \quad (1)$$

With

m = Flow rate (t/h);

F_L = critical flow factor;

C_v = valve flow coefficient (GPM);

P₁ = upstream pressure (bar abs);

T_{sh} = steam superheated temperature (°C);

y = (1.63/F_L) * √(ΔP/P₁);

If y < 1.5, subcritical flow;

if y > 1.5, then y is capped at y = y_{max} = 1.5 for critical flow;

ΔP = P₁ – P₂ with P₂ = downstream pressure (bar abs).

The important thing is not the quantitative value, but the relationship between “restricted flow”, which is shown as formula (1) and reactor pressure (or containment pressure). For example, by assuming P₁ = 1.2 × P₂ and critical flow factor F_L and steam superheated temperature T_{sh} °C are constant, the “restricted flow” m (t/h) is proportional to the containment pressure (P₂) or the reactor pressure (P₁). This implies that when the pressure was raised, the “restricted flow”, i.e., the amount of the reactions, also increased, and then increasing the amount of the reactions also increased the pressure with

increasing speed. So, once the Zr-H₂O reactions began, the reactions of the zircaloy claddings of fuel rods in the high temperature area would continue until there was no more Zr to react with.

(2) Analysis and evaluation of measured values of reactor and containment (D/W) pressures in Unit 2

Based upon the fundamental approach of Section 2.1 (1), RPV and D/W pressure changes are analyzed in Unit 2 (see to Figure 7). After 18:00 on March 14, the SRV was opened and the RPV was de-pressurized. After 20:00 (①), the Zr-H₂O reactions took place and the first rapid rise of RPV pressure started. Since this rapid pressure rise was proportional to the amount of the reactions, the pressure rise curve was almost linear. On the other hand, the D/W pressure (②) was kept constant for about 1 hour. It is presumed that a new flow route for superheated steam with hydrogen was formed in the SRV release line, and then the temperature stratification was completed in the S/C water. And most of the steam would be condensed during this 1 h. Meanwhile, an operator opened an additional SRV valve at 21:00 on March 14 (③). The opening of the second valve affected the RPV pressure immediately, and the pressure curve showed an inflection at this time. The rate of the pressure increase was decreased by opening the valve, as the rate of the reactions was decreased proportionally. On the other hand, no influence on D/W pressure appeared soon, and it appeared at about 1.5 h later, as the result of the second rapid rise ⑤ of RPV pressure after the Zr-H₂O reactions. (The pressure rise ④ 20 min after ③ was the result of completion of the flow route of ② as mentioned before.) At that time, it is presumed that the influence on D/W pressure by opening the additional SRV appeared as soon as the pressure changed because the temperature stratification had been completed in the S/C water. The D/W pressure was increasing while the RPV pressure was decreasing after ⑥. Though the RPV pressure influenced the rate of the steam and hydrogen generated by the Zr-H₂O reactions, D/W pressure influenced

their integrated or stored values, and the hydrogen and steam flow to the D/W continued after ⑥. The third rapid rise of RPV pressure was a linear increase, shown as ⑧, ⑨ and ⑩ which indicated the reaction speed increased in proportional to the pressure. During that time, it is presumed the D/W pressure was kept almost constant (⑦), as the D/W upper lid was lifted up and down slightly. At the third rapid rise of RPV pressure, the mass of hydrogen generated by the reactions could be estimated as equivalent to that of the second reaction (P value of 220 kg in Unit 2; see Figure10), and the upper lid could be lifted more during this time. Further, it is presumed that there was no RPV pressure change observed after the third rapid rise of RPV pressure, and so the difference between the RPV pressure and D/W pressure could be within the high-pressure gage error (RPV pressure was presumed to be 20% to 30% higher than the D/W pressure).

(3) Analysis and evaluation of measured values of reactor and containment pressures in Unit 3

The analysis for Unit 3 in Figures 8 and 9 (at ①, ②, and ③) can be done in the same way as for Unit 2. At ① in Figure 8, the Zr-H₂O reactions occurred, and the RPV pressure was raised and reached the set pressure of the auto de-pressurization, and the de-pressurization occurred. After that, as the reactions occurred at ② and ③ in Figure 8, the sudden RPV pressure change occurred. The pressure changes of ①, ② and ③ in Figure 9 are D/W pressure changes at the same times of the RPV pressure changes in Figure 8. In Unit 3, prior to the auto de-pressurizing of Figure 8 ①, RPV valve seat leaking had continued for a long time. As temperature stratification was produced in the S/C water and "6 SRV valves out of 8 were opened simultaneously upon receiving the auto de-pressurizing signal (Attachment 3-3, p 14 in TEPCO's 5th Progress Report)", the D/W pressures were assumed to respond and to raise immediately. After that, pressure changes of the RPV were not observed for the same reason (gage error) as in the case of Unit 2.

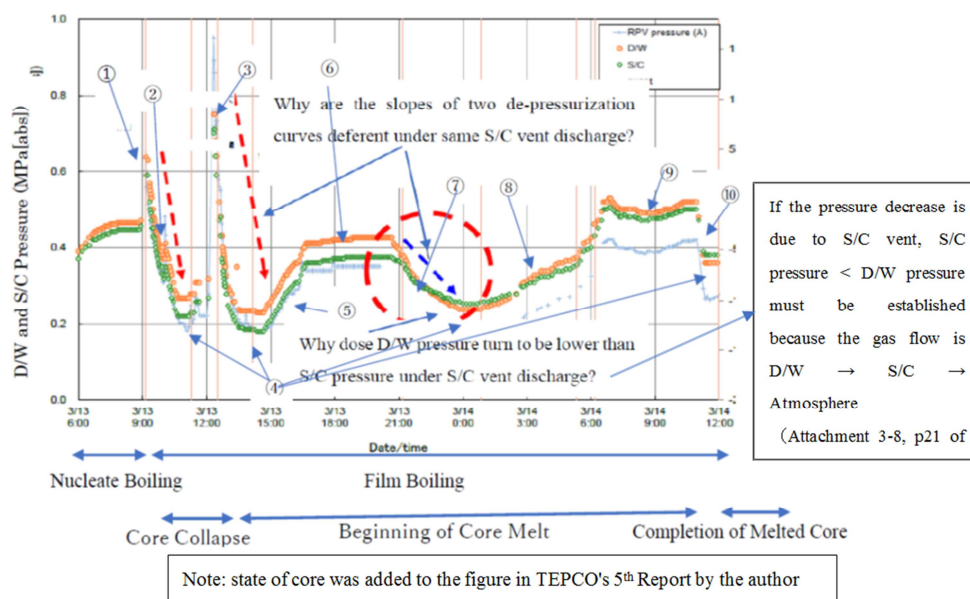


Figure 9. Containment (D/W and S/C) Pressure (expand) of Unit 3 [1].

Since the containment pressures (measured data) of both the D/W and S/C in Unit 3 were available, the analysis and evaluation were applied for the pressure rise periods, high-pressure keeping periods and de-pressurizing periods. These results were used for the basis of the mass calculation of the hydrogen generated by the reactions in Section 2.2.

At first, it is assumed that the pressure rise periods (in Figure 9: 09:00 (①), 11:00 and after (③), 14:30 and after (⑤) on March 12, and 00:00 and after (⑧) on March 13) were for film boiling with “slow and long-term reactions”. The amounts of Zr-H₂O reactions of “slow and long-term reactions” were proportional to the “restricted flow” of the steam and hydrogen. As the “restricted flow” was proportional to the pressure, the pressure curve ascended linearly or with increasing speed. The reaction speed could be estimated with the pressure gradient.

Further, heat dissipation from the containment vessel was proportional to the difference of steam saturation temperature and wall surface temperature but could not catch up to the amount of the reaction heat, which was proportional to pressure, so the difference of the heat was stored in the containment vessel, and the pressure curve had an upward tendency (Figure 9, ⑧). However, in Section 2.2 (1), for conciseness of macro evaluation, the calculation was performed with the assumption that the heat dissipation balanced with the heat storage. Then, for the high-pressure keeping periods (in Figure 9, after 16:30 on March 13 (⑥) and after 07:00 on March 14 (⑨)), the author considers that the reactions were continuing and the upper cover (lid) of the D/W was lifted and leaking began from there, and so the pressure curves had an inflection and kept the horizontal plateau with the high pressures. Since the diameter of the lid of D/W was large (about 10 meters), the change of the lid opening had a significant effect on the pressure. Furthermore, the author considers that when the pressure rise stopped, the increase in the amount of the reactions also stopped, and so the pressure changes were very large. Though the steam condenses, hydrogen does not condense by heat dissipation. The author considers that as the stored hydrogen gas leaked from the lid opening, the pressures of the D/W were kept constant at a high pressure during these periods.

Finally, for the de-pressurizing periods (in Figure 9, after 9:00 (①), after 12:30 (③) and after 20:30 (⑦) on March 13 and after 11:00 on March 14), the author considers that slow and long-term reactions ceased, and so the pressure in the containment vessel was decreased by heat dissipation. Further, the author considers that the ceasing of the reactions means the ceasing of the reactions of the high temperature Zircaloy fuel coatings and/or the surface of the melted mixtures, while the internals of the melted mixtures were kept at a high temperature by the decay heat (see Figure 1).

2.2. Calculation of Amount of Hydrogen (or Zr) Generated During Zr-H₂O Reactions

Based upon the fundamental approach of Section 2.1 (1), in which the Zr-H₂O reaction heat becomes “Input heat for

increasing and decreasing pressure” and based upon the analysis and evaluation of containment pressures during the pressure rise periods, the high-pressure keeping periods and the de-pressurizing periods in Section 2.1 (2) and (3), the amounts of hydrogen generated during the Zr-H₂O reactions were calculated as follows.

(1) Calculation of the generated hydrogen for pressure rise periods

With the assumption that the measured pressures in the containment vessel was composed of the initial pressures produced by decay heat and the pressure rises by “the heat input for increasing and decreasing steam pressure” with the Zr-H₂O reactions, the heat input by the reactions can be calculated using measured pressure changes by the reactions. The decay heat itself is large as an absolute value but is included in the initial pressures (measured values). As for the decay heat, when the next reaction starts after the first reaction, the initial pressure (at the calculation point) rises gradually due to the decay heat stored in all systems of the reactor and the containment vessel. This phenomenon is apparent from the fact that the lowest points (boiling points after de-pressurizing) of the pressures of the D/W and S/C are gradually rising (see Figure 9-④).

Now, the hydrogen and the steam generated by the Zr-H₂O reactions are considered separately for a simplified calculation. It is assumed that the containment vessel volume ($V = V_1 + V_2$ m³) is divided tentatively by the volume (V_1 ; m³) for only hydrogen and (V_2 ; m³) for only steam during the pressure rise periods, and its final pressure is the same P (MPa).

It is assumed that the pressure becomes P when the hydrogen gases of G kg are generated in the V_1 (m³) volume. As the mass and volume of hydrogen gas at the standard conditions (20°C, 0.1 MPa) are 2 kg and 22.4 m³, respectively, G can be calculated by Equation (2) with $n = PV/RT$. Mean temperature T of hydrogen gas in the containment vessel is assumed to be 200°C. Further, the following nomenclature is defined: Steam enthalpy, h'' kJ/kg; water enthalpy, h' kJ/kg; specific steam volume, v'' m³/kg; and specific water volume, v' m³/kg. It is assumed that part of the steam is generated from the water in the volume of V_2 and the state of steam and water in V_2 changes from state 1 of (h_1' , h_1'' , v_1' , v_1'') to state 2 of (h_2' , h_2'' , v_2' , v_2'') by the reaction heat of Q (kJ). The water volume in state 1, which is changed to steam in state 2, is defined as X (m³), and the steam weight in state 2 is V_2/v_2'' . The sum of the steam weight ($V_2 - X$)/ v_1'' in state 1 and the water weight X/v_1' in state 1 is the same weight as the steam weight in state 2, shown as Equation (3) based upon mass balance. The value of v_1'/v_1'' is small enough to neglect ($1 \gg v_1'/v_1''$ (0.001/0.24=0.004 at maximum)) under smaller pressures than 0.8 MPa. So, Equation (3) is simplified as Equation (4) by this deletion. On the other hand, state 1 is changed to state 2 with heat Q addition, so the enthalpy difference between state 2 and state 1 is heat Q , shown as Equation (5) based upon energy balance. Equation (4) is substituted into Equation (5) and

Equation (6) is obtained. As h_1''/h_1' is less than 6 times smaller, $h_1''/h_1' \times v_1'/v_1''$ is less than 2.4% (=less than 6×0.004) for higher pressure than 0.15 MPa. So, Equation (6) is simplified as Equation (7). Zr-H₂O reactions are given by Equation (8), since hydrogen gas of 4 g generates an energy of 586 kJ, so reaction heat is 0.147×10^6 kJ/kg. The heat (Q; kJ) required for the pressure rise is same as the reaction heat and given by Equation (9). (Tentative volumes V_1 and V_2 are got by repeated calculations.)

$$G = V_1 / 11.2 \times P / 0.1 \times 293 / T \quad (2)$$

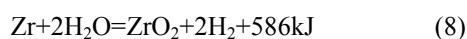
$$V_2 / v_2'' = (V_2 - X) / v_1'' + X / v_1' \quad (3)$$

$$X / v_1' = V_2 (1 / v_2'' - 1 / v_1'') \quad (4)$$

$$Q = V_2 / v_2'' \times h_2'' - \{ (V_2 - X) / v_1'' \times h_1'' + X / v_1' \times h_1' \} \quad (5)$$

$$Q = V_2 \times (h_2'' / v_2'' - h_1'' / v_1'') + V_2 (1 / v_2'' - 1 / v_1'') \times h_1' (h_1'' / h_1' \times v_1' / v_1'' - 1) \quad (6)$$

$$Q = V_2 \times \{ (h_2'' / v_2'' - h_1'' / v_1'') - h_1' \times (1 / v_2'' - 1 / v_1'') \} \quad (7)$$



$$Q = G \times 0.147 \times 10^6 \quad (9)$$

(2) Calculations for high pressure keeping periods and de-pressurizing periods

The author considers the high-pressure keeping periods and the de-pressurizing periods as follows: while reaction heat and dissipated heat were balanced during the high-pressure keeping periods, and pressure was almost constant with the D/W cover (lid) lifted, from which the generated hydrogen gas was leaking. The reaction heat is calculated by condensation heat during de-pressurizing periods just after. After stopping the Zr-H₂O reactions, de-pressurizing occurred by dissipated heat with condensation of steam, where the reaction heat = the dissipated heat = the condensed heat.

When the containment vessel (V ; m³) was de-pressurized from state 1 of h_1'' , v_1'' to state 2 of h_2'' , h_2' , v_2'' , the heat of condensation is given by Equation (10) which is equivalent to the results of Equation (7) based upon energy balance. The total condensation heat during de-pressurizing periods is converted to the heat rate (heat per hour) and this heat rate is defined as the dissipated heat rate for high pressure keeping periods, and the total reaction heat during high-pressure keeping periods can be calculated since the reaction heat rate is the same as the dissipated heat rate. Next, the amount of hydrogen generation per hour (g kg/hour) is gotten by Equation (9). Finally, the total amount of generated hydrogen (G; kg) is calculated by multiplying g by the hours of high-pressure keeping periods.

$$Q = V \times \{ (h_1'' / v_1'' - h_2'' / v_2'') - h_2' \times (1 / v_1'' - 1 / v_2'') \} \quad (10)$$

(3) Calculation examples

Calculation examples are described for the pressure rise periods, the high-pressure keeping periods and the

de-pressurizing periods of D/W and S/C pressures (Figures 9 at ⑤, ⑥ and ⑦) from 14:30 on March 13 to 00:00 on March 14.

First, a calculation example for pressure rise periods is shown. On March 13, the D/W pressure was pressurized from 0.25 MPa ($v_1''=0.746$, $h_1''=2716$, $h_1'=533$) at 14:30 to 0.42 MPa ($v_2''=0.445$, $h_2''=2740$) at 16:30, and the S/C pressure was pressurized from 0.18 MPa ($v_1''=1.0$, $h_1''=2701$, $h_1'=490$) at 14:30 to 0.36 MPa ($v_2''=0.519$, $h_2''=2733$) at 16:30. The calculation was run separately for the D/W (4000 m³) and the S/C (3000 m³). The volume of D/W was separated as V_1 of 220 m³ and V_2 of 3780 m³ (based on repeated calculations). By Equation (2), the required amount of generated hydrogen (G; kg) for pressurizing is 51 kg, and the reaction heat (Q kJ) can be obtained from Equation (9) as 7.5×10^6 (kJ). On the other hand, from Equation (7), the required amount of heat for steam pressurizing is 7.6×10^6 kJ, which is fed by the reaction heat (Q; kJ) obtained from Equation (9).

And then, the volume of S/C is separated as V_1 of 200 m³ and V_2 of 2800 m³. By Equation (2), the required amount of generated hydrogen (G; kg) for the pressurizing is 40 kg, and the reaction heat (Q; kJ) can be obtained from Equation (9) as 5.9×10^6 kJ. On the other hand, from Equation (7), the required amount of heat for steam pressurizing is 5.8×10^6 kJ, which is fed by the reaction heat (Q; kJ) obtained from Equation (9). As a result, the required amounts of hydrogen for D/W and S/C pressurizing periods during 14:30 and 16:30 on March 13 are 51 kg and 40 kg respectively.

Then, calculation examples for high-pressure keeping periods and de-pressurizing periods are shown. After pressurizing periods, the high-pressure state continued for 4 h from 16:30 to 20:30. The dissipation heat rate for the 4 h is assumed the same as for the condensation heat rate during de-pressurizing periods after 20:30, so the amount of hydrogen generated by Zr-H₂O reactions is estimated by a backward computation method.

At first, since D/W pressure was de-pressurized from 0.43 MPa ($v_1''=0.436$, $h_1''=2741$) at 20:30 to 0.25 MPa ($v_2''=0.746$, $h_2''=2716$, $h_2'=533$) at 24:00, so 8.6×10^6 kJ is obtained from Equation (10) as the condensation heat (Q; kJ).

On the other hand, since S/C pressure was de-pressurized from 0.37 MPa ($v_1''=0.505$, $h_1''=2734$) at 20:30 to 0.27 MPa ($v_2''=0.690$, $h_2''=2720$, $h_2'=543$) at 24:00, 3.5×10^6 kJ is obtained from Equation (10) as the condensation heat (Q; kJ). The total condensation heats of D/W and S/C for 3.5 h from 20:30 to 24:00 were approx. 12×10^6 kJ, and so the required generation rate of hydrogen gas was 23 kg/h (=12/0.147/3.5). The high-pressure state continued 4 h from 16:30 to 20:30, and so the total mass of hydrogen gas was 92 kg (=23×4). As the generated hydrogen gas during the pressurizing periods was determined to be 51 kg for the D/W and 40 kg for the S/C, the generated hydrogen gas of 92 kg during the high-pressure keeping periods were also thought to be distributed according to the same ratio. However, in the D/W, 92 kg of the gas was discharged from the D/W top lid opening. Therefore, 10 kg (=51+51-92) remained in the D/W

and 80 kg (=40+40) remained in the S/C and they were the partial hydrogen pressure (Figure 9 at ④ shows the lower limit at de-pressurizing, which affected the pressure difference between the D/W and S/C).

(4) Application for all cases in Units 1, 2 and 3

Typical calculation examples are shown in Section 2.2 (3), and same calculations are executed for all case ranges of Units 1, 2 and 3 (see Figures 6, 7, 8 and 9) in this section.

The calculation conditions and results are shown in Figure 10, however only the major values are described for pressure changes. As 4 kg of hydrogen reacted with 91 kg of Zr (Equation (8)), the total mass of hydrogen (and equivalent amount of zirconium) in each unit is about 1400 kg (equivalent to 32 tons zirconium), about 1700 kg (equivalent to 39 tons zirconium) and about 1900 kg (equivalent to 43 tons zirconium), respectively.

1) In Unit 1, total mass of H ₂ produced by Zr-H ₂ O reaction is 1400kg(=Zr32ton).
①1300kg(=130kg/h×10h) during K from 04:00 to 14:00 of 3/12, then D from 0.75 to 0.5MPa/ 1.0hr
②20kg(=4kg/h×4.5h) during K from 13:30 to 18:00 of 3/13
③80kg during P from 12:00 (0.16MPa) of 3/22 to 12:00(0.42 MPa) of 3/24
2) In Unit 2, total mass of H ₂ produced by Zr-H ₂ O reaction is 1700kg(=Zr39ton).
①220kg during P at 22:00 of 3/14
②1100kg(=130kg/h×8.5h) during K from 23:00 of 3/14 to 07:30 of 3/15, then D from 0.8 to 0.2MPa/ 3.5hr
③140kg during P from 12:00 to 13:00 of 3/15
④240kg during P from 06:00 to 12:00 of 3/16
3) In Unit 3, total mass of H ₂ produced by Zr-H ₂ O reaction is 1903kg(=Zr43ton).
①72kg during P at 09:00 of 3/13
②224kg during P from 11:00 to 12:30 of 3/13
③91kg during P from 14:30 to 16:30 of 3/13
④92kg(=23kg/h×4h) during K from 16:30 to 20:30 of 3/13
⑤138kg during P from 00:00 to 06:30 of 3/14
⑥1000kg(=230kg/h×4.3h) during K from 06:40 to 11:00 of 3/14, then D from 0.52 to 0.36MPa/ 0.33hr
⑦46kg during P from 12:00 to 15:00 of 3/14
⑧46kg(=31kg/h×1.5h) during K from 15:00 to 16:30 of 3/14
⑨194kg during P from 12:00 of 3/19 to 06:00 of 3/20

Figure 10. Mass of H₂ produced by Zr-H₂O reaction in Unit 1, 2 and 3 (K, D and P show Keeping high pressure, Depressurizing and Pressurizing).

On the other hand, total masses of zirconium in reactor cores of Units 1, 2 and 3 are 36 tons, 43 tons and 43 tons respectively, and almost all the zirconium must have reacted with water. Furthermore, reviewing the results of all ranges of D/W and S/C pressures in Units 1, 2 and 3, the maximum generation rate (mass) of hydrogen gas in Unit 1 (just before the hydrogen explosion) and Unit 2 is the same value of about 130 kg/h (at 0.7 MPa), but that of Unit 3 is about 230 kg/h (at 0.5 MPa) just before the hydrogen explosion, which is about 2 times of that of Units 1 and 2. So, the maximum lifting of the top lid of the D/W was shown to occur in Unit 3. This result corresponds to the test result of after-accident analysis activities, in which the D/W was pressurized slightly by several kPa(g) in Units 1 and 2, but not in Unit 3, when nitrogen gas was charged to each D/W, (Attachment 4, p. 41 in TEPCO's 5th Progress Report). When the bolts for the containment top lid of Unit 3 were loaded with the third sudden and steep pressure rise (to 7.5 MPa) without pre-heating, significant plastic deformation of the bolts might

occur.

2.3. Estimation of the Bottom Penetration Timing of the Reactor Pressure Vessel (RPV)

After several days, decay heat (and Zr-H₂O reaction heat) was reduced and at the ending of film boiling over the melted core surface, the steam film was broken (so-called transition boiling in Figure 1). Then water, the density of which is a thousand times that of steam, flowed into the melted core, then the amount of Zr-H₂O reactions increased and the RPV wall was heated rapidly and would be melted (so-called Melt Through). Therefore, the final pressurizing points on March 22~24 (Figure 6) in Unit 1, at around 12:00 on March 16 in Unit 2 (Figure 7) and on March 19~20 in Unit 3 (Figure 8) would show the times of the PRV bottom penetrations. The amounts of generated hydrogen gas were 80kg (Figure 10, Unit 1 at ③; equivalent to 1.8 tons of zirconium), 240 kg (Figure 10, Unit 2 at ④; equivalent to 5.5 tons of zirconium) and 194 kg (Figure 10, Unit 3 at ⑨; equivalent to 4.5 tons of

zirconium).

On the other hand, once the bottom of the RPV was penetrated, the radioactivities from the melted core were released directly from the D/W, not passing through water in the S/C, and then, the radioactivities were released to the outside through the opening between the upper lid and the vessel. The radioactivity level would be raised at that time. Just around this time, a rapid rise of the monitored

radioactivity level (at Plume: P4', P8, P8', P9, P9', P10 and P11 in Figure 11) occurred at the site. Further, the author presumes that the black smoke from Unit 3 on March 21 (Attachment 3-6 in TEPCO's 5th Progress Report) came from the cables burned by the melted core after penetration of the RPV bottom; an explanation for this was one of the unresolved matters in the 5th Progress Report.

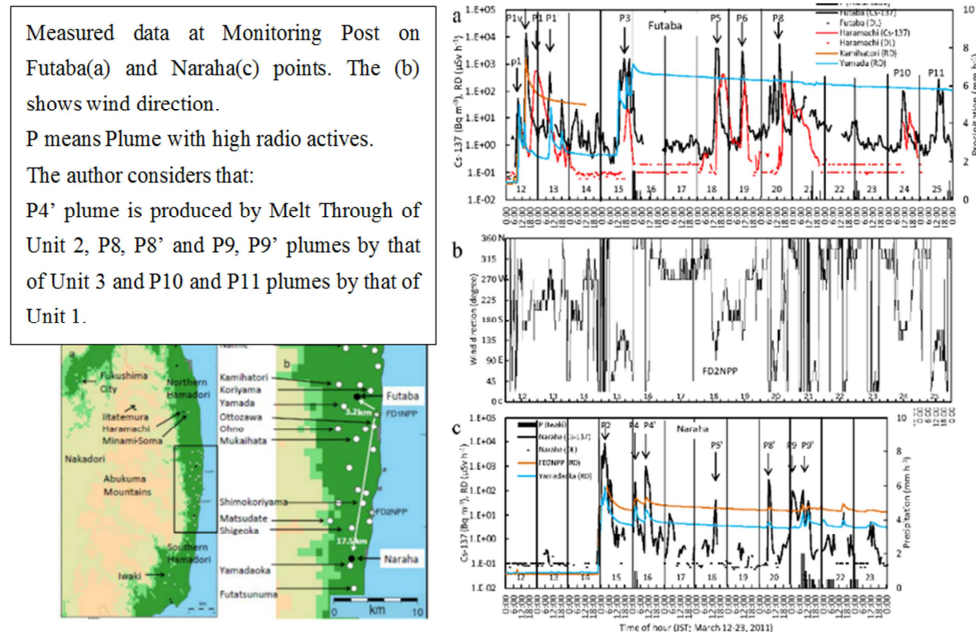


Figure 11. Radiation Dose on the Site (March 12 to 25) [5].

2.4. Re-evaluation of Measured Pressures of Reactor and Containment Vessel and Clarification of Unresolved Items [6]

The reactor cores after Zr-H₂O reactions were experiencing film boiling and the amount of the reactions was proportional to the reactor pressure. The higher the pressure, the more the amount of the reactions, followed by the pressurizing going on and on. This was one conclusion obtained from a macroscopic review and evaluation focused on the phenomena clarification. The reaction speed can be estimated by the pressure gradient. Based on this viewpoint, overall re-evaluation for the pressure transitions of the reactor and containment vessel was done for Units 1, 2 and 3. Regarding pressure transitions (Figure 9) in the containment vessel, the pressure gradients during pressurizing were becoming gentler with elapse of time. This phenomenon can be presumed that at first, the high temperature areas of the fuel claddings (Zircaloy) reacted violently, then collapsed gradually (so-called Core Collapse) and changed to a lump of molten fuel in the reactor (Beginning of Core Melt), and then the reaction speed was slowed down (Completion of Melted Core). Particularly, in the RPVs of both Units 2 and 3, sudden pressure changes (three times) from 1 to 3 MPa were observed (Figures 7 and 8). That is, the author considers that the fuel of the assemblies in the reactor core reacted violently

at three areas of the core.

During pressure rise periods, pressure curves were inflected (Figure 7 at ⑦, Figure 9 at ⑥ and ⑨). These inflections would occur because of lifting of the D/W upper lid and leaking from around its opening, and the pressure rise ceased with drop in the reaction rate by the drop in the pressure rise. These behaviors can explain the pressure transients (measured values) of Unit 2 (Figure 7) and Unit 3 (Figure 9). The upper lid lifting protected the containment vessel from the rupture by rapid over pressurizing, however, the leaking from the lid would be presumed to be huge.

On the other hand, the TEPCO 5th Progress Report [1] describes that the following phenomenon is one of the unresolved items; the pressure rises of the D/W stopped and the pressure became constant, though the sudden and steep rise of RPV pressure occurred after the third sudden pressure rises in Unit 2 (Figure 7 at ⑦, ⑧, ⑨ and ⑩), however, in the analysis of the progress report, the following is described: "TEPCO controlled and set an amount of steam and hydrogen gas in order to fit with the measured pressures of RPV and D/W" (Attachment 2-9, p. 10), such as large amounts of steam with no hydrogen gas for the reactions. This is only a computation adjustment, which does not meet the physical phenomenon.

On the contrary, the author considers that though the pressures in the RPV rose rapidly after reactions started in

the RPV, once the top lid was lifted, the pressures in the D/W were kept constant (Section 2.1 (2)). This can explain the physical phenomenon well.

Further, the important unresolved matter of “the opening and closing timings of the venting valve of S/C (for de-pressurizing and pressurizing, respectively) would not correspond to the venting time for steam and gas release based on the video records”, and the author considers that an amount of release from the venting valve is too little not to correspond to the accelerated relationship of the reactions and the pressure rise. The opening or closing of the venting valve would only give a small change to the pressure gradient and/or lifting of the top lid.

And, regarding the unresolved matter of “For almost the whole range of containment pressures in Unit 3, S/C pressures were lower than D/W pressures, though steam and hydrogen gas flowed from the S/C to the D/W”, the author considers as follows: the superheated steam and hydrogen gas from T-quencher (figures 4 and 5) through SRV flowed up in S/C water. Parts of them went into one or several pipes of 8 large pipelines (Bent pipes) which connect D/W and S/C. As the fluid density in the pipes became smaller and smaller by “chimney effect”, the flow of them increased more and more. So, D/W pressure became higher than S/C pressure by increasing of the pipeline flow with superheated steam and hydrogen gas from T-quencher, which went to D/W directly.

This can help understanding of incomprehensive phenomenon at the lowest point during de-pressurizing in Figure 9 at ④. That is, at two points of the first stage (around 10:00 and 14:00 on March 13), the vacuum breaker of the check valve (this is not described in Figure 4 but was provided in the each bypass line of 8 large connected pipes between the D/W and S/C) was closed when D/W pressure was higher than S/C pressure. On the other hand, “Around 0:00 and 11:00 on March 14, the upset phenomenon of the D/W pressure and the S/C pressure during de-pressurizing periods occurred, which is one of the unresolved matters described in Figure 9”. The author considers that this phenomenon occurred by partial pressure differences of residual hydrogen gas in D/W and S/C. The partial pressure of S/C was higher than that of D/W, from the top lid of which hydrogen gas leaked. At this time, this difference in pressure soon disappeared as the vacuum breaker of the check valve was opened (described in Section 2.2 (3)).

Though these unresolved phenomena look like inconsistent matters, they can be explained without inconsistency. Namely, pressurizing and de-pressurizing in the containment vessel were not dependent on opening and/or closing of the venting valve, but on starting and/or ceasing of the Zr-H₂O reactions and/or lifting of the top lid.

3. Discussion

In the TEPCO's 5th Progress Report [1] and other reference reports, it is described that Melt-Through of Reactor vessel occurred just after Core-Melt. But based on the author's new approach of “film boiling approach”,

Melt-Through occurred at 1 or 2 weeks after Core-Melt, shown in Figure 6, 7 and 8. Because the temperature of melted core would be more than 2000K, and steam in film boiling state would cover the melted core instantaneously. In the Progress Report, it is described that melted core could be cooled by water, which means nucleate boiling occurred immediately without passing through film boiling and transition boiling. This description does not fit to basic boiling curve shown in Figure 1. As there are many (40) unsolved matters, NRA (Nuclear Regulatory Authority) Japan began to re-review the TEPCO's 5th Reports from 2019. And also NRA has been doing site examination and sampling test and taking a video in containment vessel of Unit 1, 2 and 3. Though the following new facts were founded, NRA cannot clarify them yet and they are unsolved matters still now; first of them is that the concretes had disappeared and naked rebars appeared in the wall around the open area of the Pedestal under the RPV shown by a robot camera in the containment vessel of Unit 1 [7]. Second of them is that the radioactivity level of broken piece debris by hydrogen explosion is very low around the turbine building but is very high in the reactor building in Unit 1 and 3. Third of them is that at moment of the explosion, only the white smokes occurred in Unit 1 but the white smokes and following big spheroidal black smokes occurred in Unit 3, and so on. As these above items are clarified easily by the analysis based on “film boiling approach” (author's theory shown in Figures 6, 7 and 8), the author would like to submit the paper as verification of this approach about them in near future, after the validity of “film boiling approach” namely, “film boiling continued 1 or 2 weeks after core melt and then Melt-Through occurred during transition boiling” is recognized in this paper.

4. Conclusion

In this Commentary, the author took a macroscopic view to review the entire core melt progresses with the accompanying Zr-H₂O reactions of Units 1, 2 and 3 after loss of the core cooling function and confirmed the physical phenomena with simplified step-by-step calculations, based on measured data of reactor and containment (D/W and S/C) pressure changes. This paper provided a new approach for them. The reactor core was changed from nuclear boiling to film boiling by Zr-H₂O reaction heat (and decay heat) and the core was covered with steam and hydrogen gas and kept the film boiling state. The author assumed that the generated steam and hydrogen gas flows were restricted by flows of the SRV line (this paper called it “restricted flow”), so the reaction rate became slow for the restriction of the mass flow rate of supplied steam and the reactions continued for long time. With this “restricted flow” assumption, reactions were proportional to pressure, so the greater the pressurizing, the greater the amount of reactions, and the further the pressure was raised. Pressurizing of the D/W was restricted by leakage from the upper lid. These findings provided a good explanation for the pressure transitions of the measured data.

On the other hand, it could be supposed that a certain steam pressure was kept in the D/W and S/C, while decay heat only was consumed by sensible heat and latent heat of the core injection water. And then if Zr-H₂O reaction heat was added, the steam pressure change would be dominated by Zr-H₂O reactions. So, the containment pressure changes were dominated by Zr-H₂O reaction changes, and reactions themselves were dominated by “restricted flow”. Then, the author assumed that pressurizing of the containment vessel was dominated by the reactions, high pressure was kept by balancing with reaction heat and dissipation heat, and by leaking of hydrogen gas from the lid of the D/W, and de-pressurizing only occurred by ceasing of the reactions. Then the amount of generated hydrogen (amount of Zircaloy) could be calculated. With this extremely bold assumption, the amount of generated hydrogen gas (Zircaloy amount) was calculated using each measured value of containment vessel pressure transitions of Units 1, 2 and 3.

Further, many unresolved items in TEPCO’s 5th Progress Report were also explained reasonably. As for the macroscopic evaluation focused on phenomena understanding, explanations and analysis here were thought to be reasonable and adequate. And, with the assumption that Zr-H₂O reactions were accelerated by changing from steam to water, which covered the melted core, at the end of film boiling when decay heat was reduced, the penetration timing of the reactor vessel bottom was identified. These points were confirmed by the coincidence with the rapid changes of containment pressures of Units 1, 2 and 3 and the rapid rises of monitored radioactivity level at the site and neighboring points.

References

- [1] Tokyo Electric Power Company (TEPCO) Fifth Progress Report (<https://www.tepco.co.jp/en/decommission/accident/unsolved-e.html>)
- [2] Pool Boiling Curve - an overview | Science Direct Topics (<https://www.sciencedirect.com/topics/engineering/pool-boiling-curve>), (accessed on Oct. 08, 2021).
- [3] Main Findings, Remaining Uncertainties and Lessons Learned from the OECD/NEA BSAF Project (<https://doi.org/10.1080/00295450.2020.1724731>).
- [4] Control valves for steam, superheated steam: Calculation of Cv and mass flow (myengineeringtools.com) (<https://www.hisaka.co.jp/valve/techDoc/techDoc01.html>), (accessed on Oct. 09, 2021).
- [5] Tsuruta et al., *Geochemical Journal*, 52, 2018.
- [6] Tsuyoshi MTSUOKA, *Trans. Atomic Energy Soc. Jpn.*, Vol. 20, p131-142 (2021).
- [7] NRA Japan, Review and analysis meeting about Fukushima Daiichi Accident, the 32th Meeting (31 on November, 2022) Attachment 1-2 (Review for concrete found in PCV of Unit 1 by robot camera, Osaka University 1F-2050) (https://www.nra.go.jp/disclosure/committee/yuushikisya/jiko_bunseki01/).
- [8] *Journal of Nuclear Materials* Volume 542, 15 December 2020, 152471 Morphology and phase distributions of molten core in a reactor vessel.
- [9] Masaki Kurata, *Trans. Atomic Energy Soc. Jpn.*, Vol. 65, No. 1 p13-18 (2023).
- [10] *Nuclear Engineering and Design* Volume 403, March 2023, 112142, Development of PWR lower head failure model for severe accident analysis.
- [11] *Nuclear Engineering and Design* Volume 392, June 2022, 111746 Evaluation of temperature and flow area variations through the fuel degradation and relocation of the SFD Test 1–4, Koji Nishida.
- [12] *Journal of Hazardous Materials* Volume 428, 15 April 2022, 128214, Volatilization of B₄C control rods in Fukushima Daiichi nuclear reactors during meltdown, Kazuki Fueda.
- [13] *Journal of Nuclear Materials* Volume 572, 15 December 2022, 154040, Fission products chemistry in simulated PWR fuel up to 2100°C: Experimental characterization and TAF-ID modelling. E. Geiger.
- [14] *Journal of Nuclear Materials* Volume 559, February 2022, 153415, Research on the nuclear fuel rods melting behaviors by alternative material experiments.
- [15] *Progress in Nuclear Energy* Volume 108, September 2018, Pages 398-408, Results of simulant effect on large corium pool behavior based on COPRA facility.